Urban Extraction Based on Scattering Decomposition Using PolSAR Data

Siriprathan Y.[1*], Susaki J.[2], Ishii Y.[3], and Oba T.[4]

[1]Student, Graduate School of Engineering, Kyoto University, Japan

[2]Professor, Graduate School of Engineering, Kyoto University, Japan

[3]Assistant Professor, Graduate School of Engineering, Kyoto University, Japan

[4]Professor, Graduate School of Management, Kyoto University, Japan

*siriprathan.yasumin.64u@st.kyoto-u.ac.jp (*Corresponding author's email only)

Abstract *Urban area extraction and classification are essential for effective urban planning, environmental monitoring, and disaster management. Traditional optical sensors, which depend on sunlight for imaging, often encounter limitations due to adverse atmospheric conditions such as cloud cover and varying light levels. These limitations can lead to incomplete or inaccurate data, particularly in regions that frequently experience weather disturbances. In contrast, Synthetic Aperture Radar (SAR) sensors provide consistent and reliable imaging capabilities, regardless of weather conditions or time of day, making them invaluable tools for urban studies, especially in challenging environments. This study leverages the capabilities of Polarimetric SAR (PolSAR) data, which uses multiple polarizations to enhance urban feature extraction through advanced scattering decomposition techniques. We propose a novel approach for urban extraction using PolSAR data, with a focus on promoting sustainable urban development through the optimized use of energy and resources. The methodology involves collecting microwave scattering data from concrete blocks at various angles within an anechoic chamber, which is then used to train machine learning models. These models are subsequently applied to real-world satellite data from ALOS-2/PALSAR-2, ensuring the practical applicability of the approach. The study employs Yamaguchi's decomposition model, utilizing the four-component scattering power decomposition method to accurately categorize urban features. Initial results demonstrate that incorporating scattering decomposition improves urban classification accuracy compared to using only raw channel data. Furthermore, the inclusion of the Polarimetric Orientation Angle (POA) enhances classification accuracy by adjusting for angular effects influenced by the radar's look angle and the orientation of structures. Validation against comprehensive real-world reference datasets confirms the robustness and wide-ranging applicability of the developed model. The results suggest that our method could be a valuable tool for urban planners and policymakers, providing them with accurate, up-to-date information on urban areas. This approach not only supports more informed decision-making but also contributes to more sustainable and efficient urban planning practices.*

Keywords: *urban area extraction, polarimetric SAR, scattering decomposition, machine learning, polarimetric orientation angle*

Introduction

The rapid urbanization occurring globally, especially in densely populated regions like Asia, poses significant challenges such as inadequate infrastructure, environmental degradation, and heightened vulnerability to natural disasters. As cities expand, there is an increasing need for effective urban mapping to support sustainable urban planning, environmental management, and disaster preparedness (Kajimoto & Susaki, 2013).

Traditional methods of urban mapping, which often rely on Geographic Information Systems (GIS) data, can be labor-intensive and slow to update, particularly in fast-growing urban areas (Li et al., 2014).

In light of these challenges, Synthetic Aperture Radar (SAR) has emerged as a powerful tool for urban analysis, providing detailed spatial information regardless of weather conditions or time of day (Yamaguchi et al., 2005). SAR's ability to penetrate cloud cover and deliver consistent imaging makes it particularly suitable for urban monitoring (Schneider et al., 2010). Polarimetric SAR (PolSAR) further enhances this capability by employing multiple polarization channels, which allow for a more nuanced interpretation of the scattering properties of urban surfaces (Niu & Ban, 2013).

Recent research has demonstrated the potential of PolSAR in urban area extraction and classification. By leveraging the unique scattering characteristics of man-made structures, these techniques enable more precise mapping of urban environments (Freeman & Durden, 1998). However, the complexity of backscattering mechanisms in urban areas presents ongoing challenges. Traditional approaches, often reliant on single-band or mono-polarized SAR imagery, have shown limitations in accurately distinguishing between various urban features (Shabou et al., 2012).

This study introduces a novel methodology for urban extraction that integrates PolSAR data with advanced scattering decomposition techniques. Specifically, we utilize the four-component scattering power decomposition method based on Yamaguchi's model to enhance the accuracy of urban feature classification (Yamaguchi et al., 2006). Additionally, we incorporate the Polarimetric Orientation Angle (POA) as a critical feature in our model. The POA, which reflects the orientation of structures relative to the radar sensor, is known to significantly influence backscattering intensity (Kimura, 2008). Correcting for POA effects can mitigate angular dependency in scattering intensity, thereby yielding more robust urban mapping results (Kajimoto & Susaki, 2013).

To further improve our urban extraction capabilities, we employed random forest classification to analyze microwave scattering data collected from concrete blocks at various angles in an anechoic chamber. This experimental dataset, provided by Niigata University, includes measurements of HV, VH, VV, and HH polarizations and serves as a foundation for training machine learning models. These models were then validated against real-world satellite data from ALOS-2/PALSAR-2. The integration of POA correction is expected to enhance the model's performance, leading to more accurate and reliable urban extraction outcomes (Ferretti et al., 2011). This research contributes to the advancement of remote sensing techniques for urban analysis, with potential applications in urban planning, resource management, and disaster risk reduction (Chaussard et al., 2014).

The remainder of this paper is organized as follows: Section 2 describes the indices employed in the proposed methodology, including the scattering matrix (S-matrix), coherency matrix (T-matrix), four-component decomposition, Polarimetric Orientation Angle (POA) estimation, K-means clustering, and Random Forest classification. Section 3 details the methodology, covering the datasets used (experimental PolSAR data and ALOS-2/PALSAR-2), and the methods applied (training dataset preparation, classification using raw channels, classification using scattering decomposition, classification using scattering decomposition combined with POA, hyperparameter tuning, and validation method). Section 4 presents and discusses the classification results, including those from classification using raw channels, scattering decomposition, and the combined approach with POA, along with an analysis of omission and commission errors. Finally, Section 5 provides conclusions and recommendations for future research.

Indices Used

In this section, we discuss the various indices used in the study for urban extraction and classification using Polarimetric SAR (PolSAR) data. These indices include the scattering matrix (S-matrix), the coherency matrix (T-matrix), the four-component decomposition, the Polarimetric Orientation Angle (POA) estimation, the K-means clustering, and the Random Forest classification algorithm. Each index plays a crucial role in enhancing the accuracy of urban feature extraction and classification.

a. Scattering Matrix (S-matrix):

The scattering matrix is fundamental in describing the scattering behavior of a target in PolSAR. It captures the complex amplitudes of the scattered field in different polarizations. For a monostatic radar system, the scattering matrix S is expressed as:

$$S = \begin{pmatrix} S_{HH} & S_{HV} \\ S_{VH} & S_{VV} \end{pmatrix} \tag{1}$$

Where S_{HH} and S_{VV} represent the co-polarized backscatter for horizontal and vertical polarizations, respectively, while S_{HV} and S_{VH} represent the cross-polarized backscatter, for simplicity, S_{HV} and S_{VH} are assumed to be equivalent. The scattering matrix forms the basis for further decomposition and classification methods.

b. Coherency Matrix (T-matrix):

The coherency matrix T is derived from the scattering matrix and represents the second-order statistics of the scattering mechanism. It is beneficial for characterizing the scattering properties in terms of power and correlation. The coherency matrix is given by:

$$T = \begin{pmatrix} T_{11} & T_{12} & T_{13} \\ T_{21} & T_{22} & T_{23} \\ T_{31} & T_{32} & T_{33} \end{pmatrix}$$

$$= \begin{pmatrix} \frac{\langle |S_{HH}+S_{VV}|^2 \rangle}{2} & \frac{\langle (S_{HH}+S_{VV})(S_{HH}-S_{VV})^* \rangle}{2} & \langle (S_{HH}+S_{VV}) S^*{}_{HV} \rangle \\ \frac{\langle (S_{HH}+S_{VV})^*(S_{HH}-S_{VV}) \rangle}{2} & \frac{\langle |S_{HH}-S_{VV}|^2 \rangle}{2} & \langle (S_{HH}-S_{VV}) S^*{}_{HV} \rangle \\ \langle (S_{HH}+S_{VV})^* S_{HV} \rangle & \langle (S_{HH}-S_{VV})^* S_{HV} \rangle & \langle 2|S_{HV}|^2 \rangle \end{pmatrix} \tag{2}$$

This matrix provides a comprehensive description of the scattering process by considering the coherency and phase differences between polarizations. The elements of the matrix correspond to different scattering mechanisms: T_{11} for surface scattering, T_{22} for double-bounce scattering, and T_{33} for volume scattering (Yamaguchi et al., 2020). Other elements contribute to less physically defined scattering processes, such as T_{12}, T_{13}, and T_{23}.

c. Four-Component Decomposition:

The four-component decomposition technique involves breaking down the observed backscattering into four distinct components derived from the coherency matrix (Yamaguchi et al., 2006). When this method is applied to the full PolSAR dataset, it yields the surface scattering power (*Ps*), double-bounce scattering power (*Pd*), volume scattering power (*Pv*), and helix scattering power (*Ph*). It's important to note that these components are also influenced by the Polarimetric Orientation Angle (POA).

To address this, Yamaguchi et al. (2006) introduced an approach that rotates the coherency matrix based on the POA, which helps mitigate the dependence of these components on the relative azimuth. The rotation applied to the coherency matrix can be expressed as:

$$T(\theta) = \begin{pmatrix} T_{11}(\theta) & T_{12}(\theta) & T_{13}(\theta) \\ T_{21}(\theta) & T_{22}(\theta) & T_{23}(\theta) \\ T_{31}(\theta) & T_{32}(\theta) & T_{33}(\theta) \end{pmatrix} = \left[R_p(\theta)\right]^{\dagger} \cdot T \cdot R_p(\theta) \tag{3}$$

Where P_{surface}, $P_{\text{double-bounce}}$, P_{volume}, and P_{helix} represent the power contributions of surface, double-bounce, volume, and helix scattering mechanisms, respectively (Yamaguchi et al., 2006). In this equation, † signifies complex conjugation and transposition, while $R_p(\theta)$ represents the rotation matrix defined as:

$$R_p(\theta) = \begin{pmatrix} 1 & 0 & 0 \\ 0 & cos2\theta & sin2\theta \\ 0 & -sin2\theta & cos2\theta \end{pmatrix} \tag{4}$$

d. Polarimetric Orientation Angle (POA) Estimation:

The Polarimetric Orientation Angle (POA) is crucial for accurately representing the orientation angle of target structures relative to the radar's line of sight. POA can be estimated using the following equation:

$$\theta = \frac{1}{4}\tan^{-1}\left(\frac{2Re(\langle T_{23}\rangle)}{\langle T_{22}\rangle - \langle T_{33}\rangle}\right), \left(-\frac{\pi}{4} \leq \theta \leq \frac{\pi}{4}\right) \tag{5}$$

Where Re denotes the real part of the complex number, and T_{22}, T_{23}, and T_{33} are elements of the coherency matrix. Incorporating POA into the classification model is essential for improving the accuracy of urban feature extraction, as it corrects angular effects caused by the orientation of structures (Kajimoto & Susaki, 2013).

The POA can be conceptualized as the angle of rotation around the radar's line of sight. The transformation of a scattering matrix rotated by an orientation angle ξ is represented as:

$$S(\xi) = \begin{pmatrix} cos\xi & sin\xi \\ -sin\xi & cos\xi \end{pmatrix}\begin{pmatrix} S_{HH} & S_{HV} \\ S_{VH} & S_{VV} \end{pmatrix}\begin{pmatrix} cos\xi & -sin\xi \\ sin\xi & cos\xi \end{pmatrix} \tag{6}$$

In reflection-symmetric media like horizontal surfaces, the POA is typically zero (Lee et al., 2000). However, in steep terrains or urban environments, the POA often deviates from zero due to surfaces with non-zero azimuth slopes and man-made structures that are not aligned with the radar’s flight direction, such as buildings and bridges with inclined features (Lee et al., 2002). Understanding and incorporating these shifts in POA is crucial for accurate terrain modeling and urban classification, leading to more reliable results (Ainsworth et al., 2008).

e. K-means Clustering

The K-means clustering algorithm can be defined mathematically as follows:

$$J = \sum_{i=1}^{k}\sum_{j=1}^{n}\left\|x_j - \mu_i\right\|^2 \tag{7}$$

Where:

n: total number of data points in the dataset.

J: objective function to minimize.

k: number of clusters.

x_j: data point.

μ_i: centroid of cluster i.

K-means clustering was selected for its simplicity, efficiency, and ability to dynamically classify urban and non-urban areas for experimental datasets without the need for manual labeling.

f. Random Forest Classification:

The Random Forest algorithm is used as a machine learning classifier to categorize urban features based on the indices discussed. It is an ensemble learning method that constructs multiple decision trees during training and outputs the class that is the mode of the classes (for classification) or the mean prediction (for regression) of the individual trees. This algorithm is particularly effective in handling high-dimensional data and capturing complex interactions between features (Breiman, 2001).

Methodology

This study focuses on urban extraction and classification using Polarimetric Synthetic Aperture Radar (PolSAR) data, divided into three key stages: classification using raw channels, classification using full polarizations (HV, VH, VV, and HH), and classification using scattering decomposition combined with Polarimetric Orientation Angle (POA). The methodology is structured into two primary subsections: data and method. This section provides detailed information on the datasets used, the preprocessing steps taken, and the methods applied in this study.

a. Data

a.1. Experimental PolSAR Data

The experimental dataset consists of backscattering measurements at various orientation angles and distances recorded in an X-band frequency. The data was collected using a fully polarimetric SAR system in an anechoic chamber at Niigata University. The key polarizations considered are HH, HV, VH, and VV, which are essential for urban extraction and classification tasks. This experimental data helps enhance the accuracy of the model by providing precise scattering characteristics, particularly for urban areas. The simulation involved measurements on concrete blocks, with sizes determined using the law of similarity, ensuring that the experiment realistically represents real-world conditions.

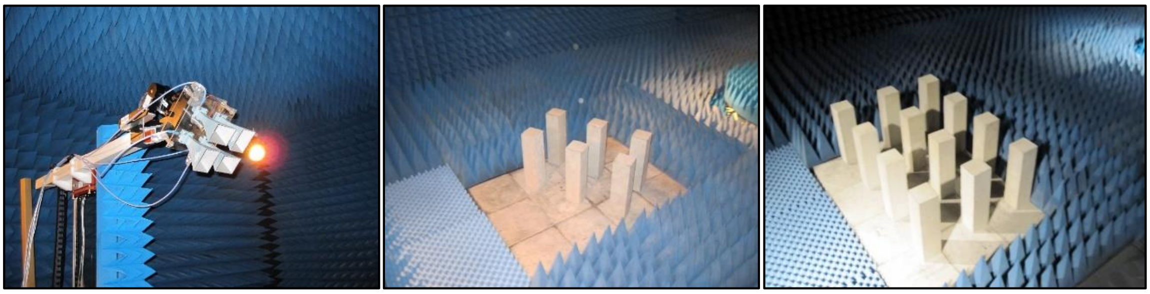

Figure 1: Setting up the microwave scattering measurement experiment dataset in an anechoic chamber at Niigata University.

a.2. ALOS-2/PALSAR-2

The ALOS-2/PALSAR-2 dataset, operated by JAXA and utilizing an L-band frequency (1.27 GHz), was employed for large-scale urban mapping in the Tokyo area. This study utilized data acquired on May 7, 2024, with an ascending orbit (scene ID: ALOS-2_PALSAR-2_ALOS2537680710-240507) and an off-nadir angle of 25.0 degrees. The dataset features a high spatial resolution of 6 meters and captures crucial polarimetric information, including both amplitude and phase data. This polarimetric data is vital for distinguishing between urban and non-urban areas, as it provides detailed insights into surface characteristics such as roughness and dielectric properties. The ability of ALOS-2/PALSAR-2 to operate in various polarimetric modes (e.g., HH, HV, VV) enhances its sensitivity to different surface types, making it particularly effective for urban classification tasks. The data's high resolution and polarimetric capabilities make it a powerful tool for urban feature extraction and analysis.

b. Method

b.1. Training Dataset Preparation

The training dataset for this study is derived from experimental PolSAR data measurements conducted at Niigata University, which includes microwave scattering data collected from concrete blocks at various azimuth angles. The dataset includes approximately over 600,000 pixels for both the non-urban and urban classes, ensuring balanced representation and minimizing bias. Data normalization techniques were applied to address any imbalanced features. Initially, K-means clustering was employed to identify natural groupings within the data, which were then used to label the urban and non-urban classes. These labeled data points served as the foundation for subsequent model training. Figure 2 shows the scattering X-band experimental data and the clustering results, where (a) represents HH, (b) HV, (c) VV, and (d) the classification results.

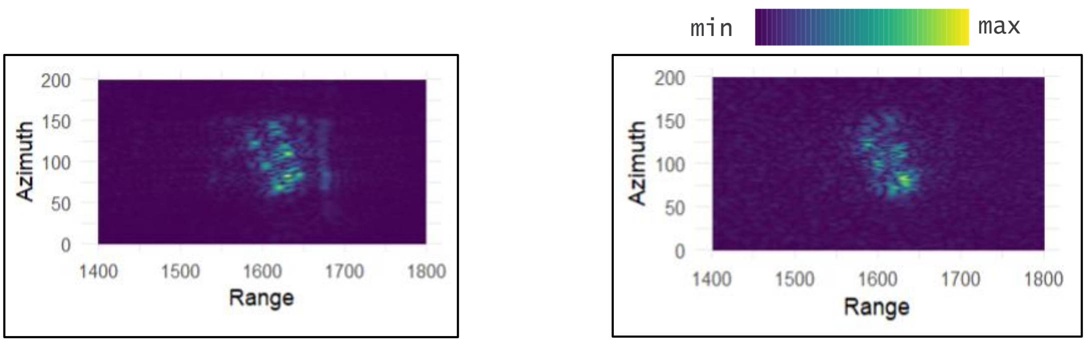

(a) [-72, -30 dB]　　(b) [-67, -31 dB]

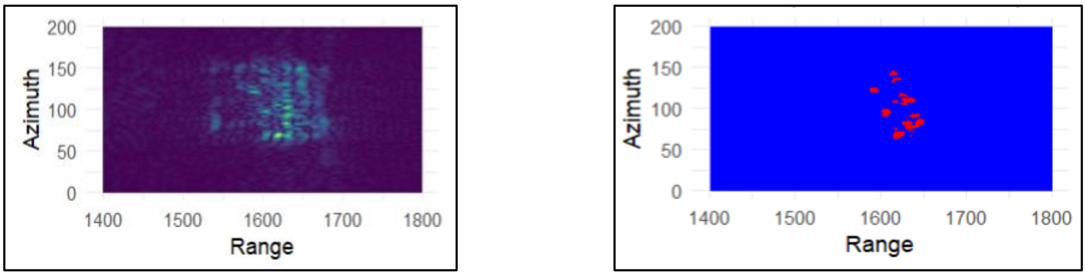

(c) [-71, -29 dB] (d)

Figure 2: Scattering x-band experimental data and clustering results for urban classification. (a) HH, (b) HV, (c) VV, and (d) classification (red pixels denote urban areas, and blue pixels denote nonurban areas).

b.2. Classification Using Raw Channels

The initial step in our methodology involves the direct classification of urban areas using raw PolSAR data channels: HV, VH, VV, and HH. These channels, representing the horizontal and vertical polarization states, contain vital information about the backscatter from various urban features. Each pixel's intensity in these channels reflects the strength of the radar signal, which interacts with objects in the scene. A Random Forest classifier was trained using these raw data channels to establish a baseline for urban feature classification. This approach allows us to evaluate the discriminative power of the raw channels in distinguishing between different urban and non-urban classes without additional feature extraction.

b.3. Classification Using Scattering Decomposition

In the next phase, we apply the four-component scattering decomposition technique, based on Yamaguchi's decomposition model, to the PolSAR data. This technique decomposes the SAR signal into four scattering mechanisms: surface scattering (*Ps*), double-bounce scattering (*Pd*), volume scattering (*Pv*), and helix scattering (*Ph*). By using these decomposed components as features in our Random Forest classifier, we aim to improve the classification accuracy by capturing more detailed physical characteristics of urban areas, which are often mixed and complex in nature.

b.4. Classification Using Scattering Decomposition + POA

The third stage of the methodology introduces an advanced classification technique that integrates scattering decomposition with POA as an additional feature. Scattering decomposition techniques, such as the Yamaguchi four-component model, decompose the PolSAR data into distinct scattering mechanisms: surface scattering (*Ps*), double-bounce scattering (*Pd*), volume scattering (*Pv*), and helix scattering (*Ph*). By incorporating POA into the decomposition process, we aim to correct for orientation-induced distortions, which are prevalent in urban areas due to the varied alignment of structures. The classifier, now trained with *Ps*, *Pd*, *Pv*, *Ph*, and POA, is expected to yield more accurate urban feature extraction by accounting for both the scattering characteristics and the orientation of urban features. Figure 3 presents a flowchart of the proposed study, outlining the methodology followed in each stage.

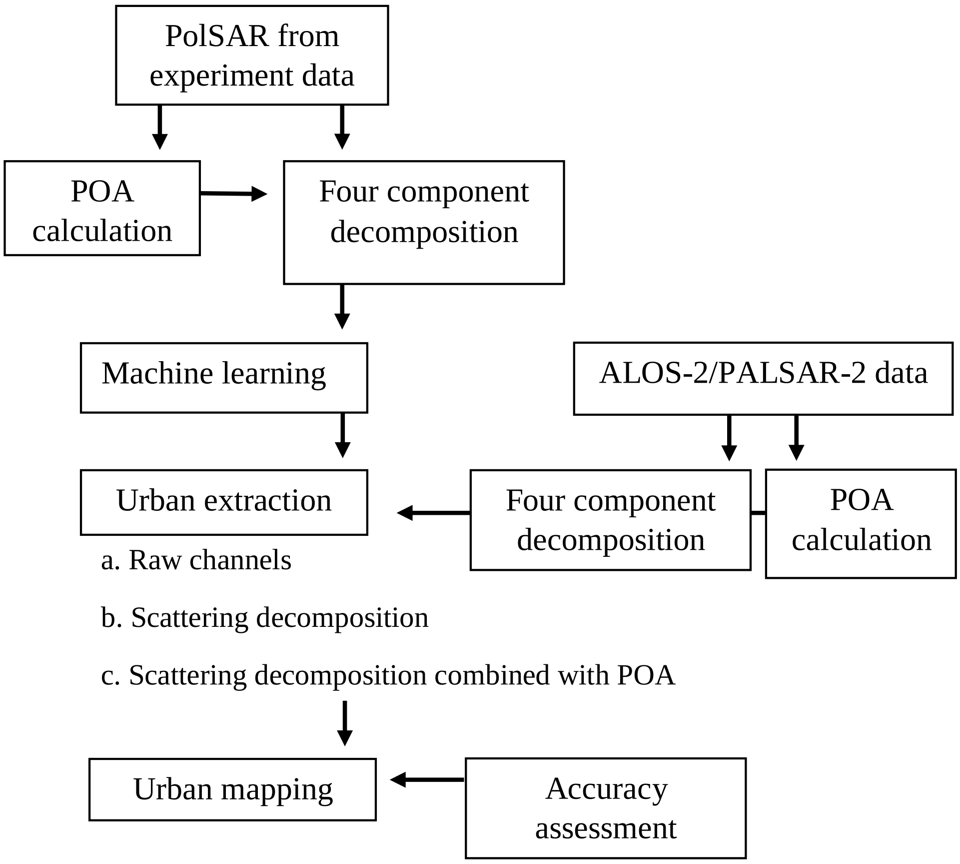

Figure 3: Flowchart of the proposed study.

b.5. Hyperparameter Tuning

The Random Forest (RF) model used in the classification stages underwent hyperparameter tuning using a Random Search approach. The primary hyperparameters adjusted were mtry, which represents the number of variables randomly sampled as candidates at each split, and ntree, the number of trees in the forest. For mtry, a tuning range of 2 to 10 was explored, while for ntree, the range was set between 50 and 200. While increasing ntree can improve performance, it also raises computation time; in this study, mtry was set to 2, and ntree to 100. These parameters were selected based on preliminary experiments to optimize the model's performance.

b.6. Validation Method

The validation of the classification results was performed by comparing the ALOS-2/PALSAR-2 derived urban maps with the Sentinel-2 land cover dataset, recognized for its 10-meter resolution. To address the resolution discrepancy between the ALOS-2/PALSAR-2 data (6 meters) and the Sentinel-2 data (10 meters), a nearest neighbor resampling technique was applied, ensuring accurate pixel-to-pixel correspondence. The Sentinel-2 land cover data, produced annually using a deep learning AI model and a vast training dataset, served as a reliable reference for validation (Karra et al., 2021)

The accuracy assessment was conducted by calculating Overall Accuracy (OA), Producer's Accuracy (PA), and User's Accuracy (UA) for both urban and non-urban classes. The results were further analyzed to identify areas of omission and commission errors, with a specific focus on regions where the ALOS-2/PALSAR-2 classification may have misinterpreted urban features due to similar scattering characteristics.

Results and Discussion

This study investigates urban extraction and classification using Polarimetric Synthetic Aperture Radar (PolSAR) data, focusing on the performance of various classification techniques. We evaluated the results using a comprehensive ground truth dataset from Sentinel-2, which provides 10-meter land cover data for 2023 (Karra et al., 2021). The classification methods employed include classification results, classification using raw channels, classification using scattering decomposition, classification using scattering decomposition combined with the Polarimetric Orientation Angle (POA), omission and commission error analysis, and a proposed method with comparisons.

a. Result of Classification

The classification of urban areas was carried out using three different approaches:

a) Raw channels: Using the original PolSAR data channels without any decomposition.

b) Scattering decomposition: Utilizing a scattering decomposition method to enhance the classification.

c) Scattering decomposition combined with Polarimetric Orientation Angle (POA): Integrating POA with scattering decomposition to further improve classification accuracy.

Each method's performance was assessed using Producer's Accuracy (PA), User's Accuracy (UA), and Overall Accuracy (OA), providing comprehensive insights into their effectiveness. A ground truth dataset derived from Sentinel-2 10-meter Land Cover data for 2023 was employed for validation (Karra et al., 2021).

Table 1: Classification accuracy results for different methods.

Classification Method	**PA [%]**	**UA [%]**	**Overall Accuracy [%]**
a) Raw channels	85.82	80.70	84.34
b) Scattering decomposition	87.03	81.99	85.57
c) Scattering decomposition + POA	88.64	84.32	87.89

Table 1 summarizes the classification accuracy results for the different methods, demonstrating that incorporating scattering decomposition and POA significantly enhances the accuracy of urban classification using PolSAR data. The highest accuracy was observed with the combined approach, making it the most reliable method for urban extraction in this study. Figure 4 displays the results of urban classification for the satellite ALOS-2/PALSAR-2 over the Tokyo area, with (a) showing urban estimation using raw channels, (b) urban estimation using scattering decomposition, and (c) urban estimation using scattering decomposition combined with POA.

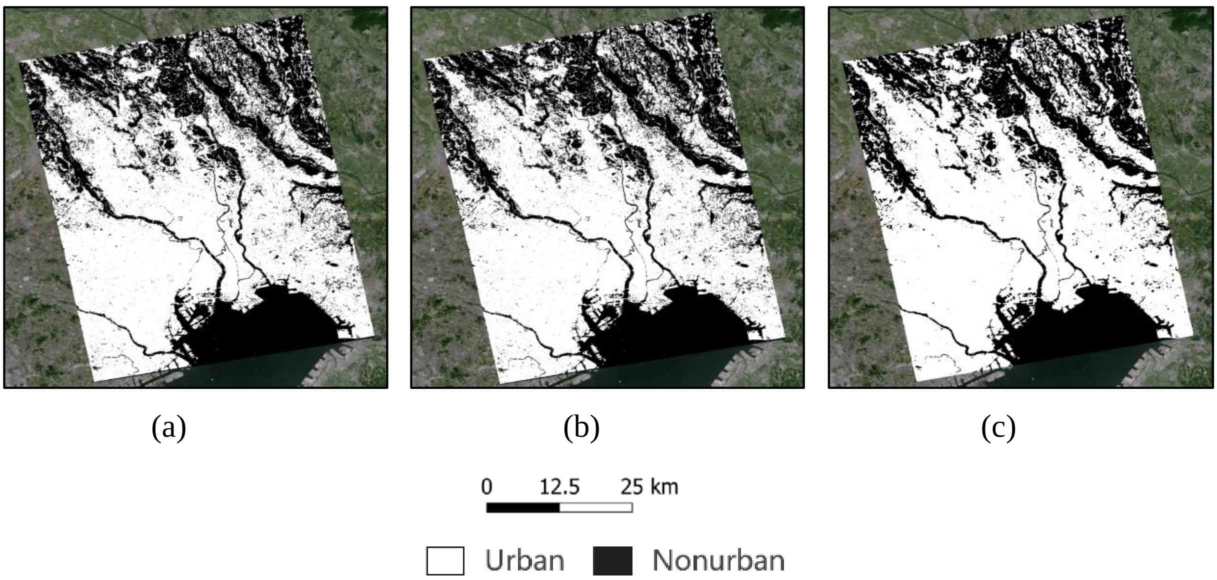

Figure 4: Results of urban classification for Tokyo, (a) urban estimation using raw channels, (b) urban estimation using scattering decomposition, (c) urban estimation using scattering decomposition + POA.

b. Classification Using Raw Channels

The initial classification approach utilized the raw channels of PolSAR data, serving as a foundational method for urban classification. The results, summarized in Table 1, indicate an overall accuracy of 84.34%. The overall Producer's Accuracy (PA) was recorded at

85.82%, while the User's Accuracy (UA) reached 80.70%. This discrepancy between PA and UA suggests that while many features classified as urban were correctly identified, some misclassification occurred, particularly with non-urban features being mislabeled as urban.

The limitations of using raw channel data stem from its inability to fully capture the intricate scattering characteristics that define urban environments. Urban areas are complex, featuring a mix of materials and structures that produce diverse scattering responses. The raw channel classification, while beneficial as a baseline, may lack the sensitivity needed to accurately differentiate these nuances, resulting in potential misclassifications that can impact urban planning and analysis.

c. Classification Using Scattering Decomposition

To enhance classification performance, the study employed scattering decomposition, leveraging the polarimetric characteristics inherent in SAR data. This method yielded an overall accuracy of 85.57%, with an overall PA of 87.03% and a UA of 81.99%. The improvements observed in both PA and overall accuracy underscore the effectiveness of scattering decomposition in urban classification.

The increased PA indicates a more precise identification of urban features, suggesting that this method effectively captures the unique polarimetric signatures associated with different urban structures. By analyzing the scattering mechanisms, this approach reduces confusion between urban and non-urban areas, allowing for a clearer distinction based on the physical properties of the features being classified. The ability to discern between various scattering types—including surface, volume, and double-bounce scattering—enables a more accurate representation of the urban landscape.

d. Classification Using Scattering Decomposition + POA

The third classification approach combined scattering decomposition with Polarimetric Orientation Angle (POA) estimation, aiming to further refine the classification process. This method achieved the highest overall accuracy of 87.89%, with an overall PA of 88.64% and a UA of 84.32%. The significant increase in PA indicates that this method was particularly effective in correctly identifying all classes.

The inclusion of POA is instrumental in enhancing classification accuracy, as it provides critical information regarding the orientation of target structures. Urban environments often consist of varied and complex geometries, which can lead to misclassification when traditional methods are employed. By incorporating orientation information, the classifier is better equipped to distinguish between urban and non-urban features, ultimately leading to more precise classifications. This method not only improves the accuracy of urban feature identification but also enhances the overall understanding of urban morphology and layout.

e. Omission and Commission Error Analysis

The analysis of omission and commission errors provides important insights into the classification model’s limitations in accurately identifying urban features. Figure 5 displays the omission and commission error maps, visually representing the areas where misclassifications occurred within the study area.

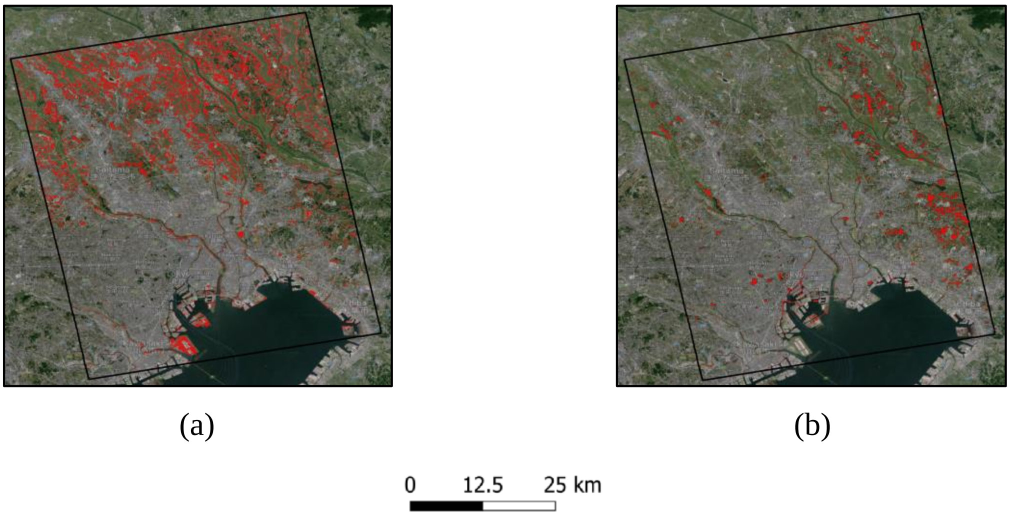

Figure 5: Omission and commission maps, (a) omission map, (b) commission map (red pixels denote misclassification areas).

e.1. Omission Errors

The omission error map (Figure 5(a)) highlights regions that should be classified as urban but are incorrectly predicted as non-urban. These errors are most common in areas with flat concrete or asphalt surfaces, such as roads, airports, and parking lots. Despite the absence of vertical structures typically associated with urban environments, these areas are integral parts of the urban landscape. The model struggles to recognize these features as urban, resulting in their misclassification as non-urban.

For instance, in Figure 6(a-d), which focuses on the Haneda airport area, the omission errors are clearly visible. The model has incorrectly classified significant portions of the airport boundary (outlined in red) as non-urban due to the flat surfaces and lack of prominent vertical structures. This example illustrates a critical limitation in the model's ability to accurately classify urban areas, especially in regions like airports that do not conform to the typical urban profile.

e.2. Commission Errors

Conversely, the commission error map (Figure 5(b)) shows that many misclassification errors result from the misinterpretation of scattering mechanisms. Specifically, areas that should have been classified as vegetation or forest (characterized by volume scattering, *Pv*) were incorrectly labeled as urban. This issue arises mainly from the limitations of traditional scattering models, which often struggle to interpret the scattering mechanisms of oriented man-made structures. These models tend to misclassify the scattering signatures of such structures as volume scattering, leading to an overestimation of urban areas in the classification output.

This issue is particularly pronounced in environments where man-made structures have varied orientations, causing mixed and noisy scattering mechanisms. The rotation of the orientation angle further complicates the interpretation of scattering, leading to the erroneous classification of non-urban areas as urban. For instance, in Figure 6(e-h), which includes parks such as Yoyogi Park, Meiji Jingu Shrine, and Shinjuku Gyoen National Garden, the commission errors are apparent where the model misclassified areas of natural vegetation (which should be black) as urban (white). These errors highlight the challenges the model faces in accurately distinguishing between urban and non-urban features in complex environments.

e.3. Proposed Method and Comparisons

Figure 6(a) shows the results from the proposed method, which exhibits only a slight improvement over the other two methods but still suffers from considerable misclassification errors. When compared with Figure 6(b), which represents classification using raw channels, and Figure 6(c), which represents classification using scattering decomposition, it becomes clear that while the proposed method reduces the number of errors slightly, it still fails to accurately delineate urban boundaries in many areas. Figure 6(d) offers an optical image from Google Earth for reference, displaying the actual extent of the airport boundary.

Despite the proposed method's slight improvement, it is clear that substantial misclassification remains, particularly in areas where traditional models also struggle. These findings suggest that while some progress has been made, there is still a significant need for more advanced models capable of better handling the complexities of urban environments, including varied orientations of man-made structures and flat, non-vegetative surfaces.

Overall, these results highlight the ongoing challenges in urban feature extraction using current classification methods. The slight improvement provided by the proposed method suggests that while there has been progress, significant work remains. Developing more sophisticated models that can more accurately distinguish between different scattering mechanisms, especially in complex urban environments, will be essential. Enhancing the classification process to better account for the diversity of urban structures and surfaces will be crucial for improving the accuracy of urban area extraction.

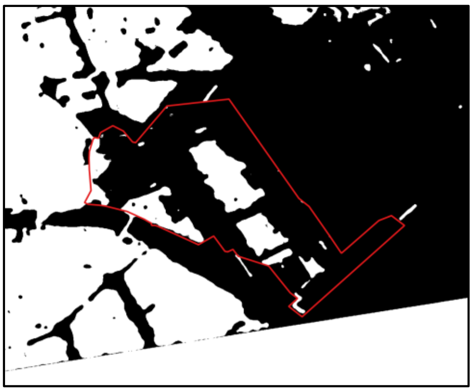

(a)

(b)

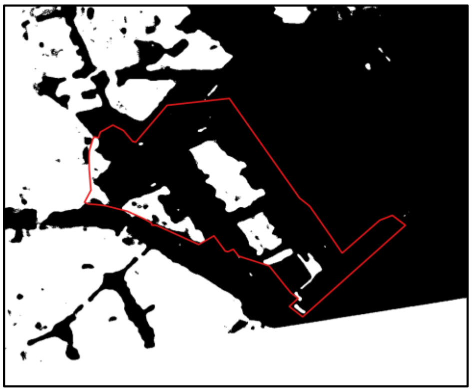

(c)

(d)

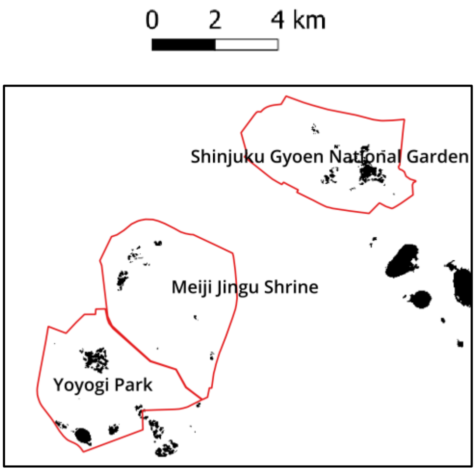

(e)

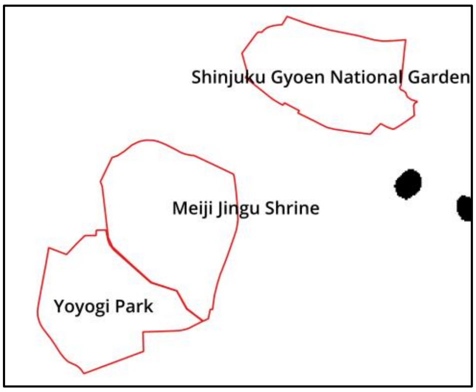

(f)

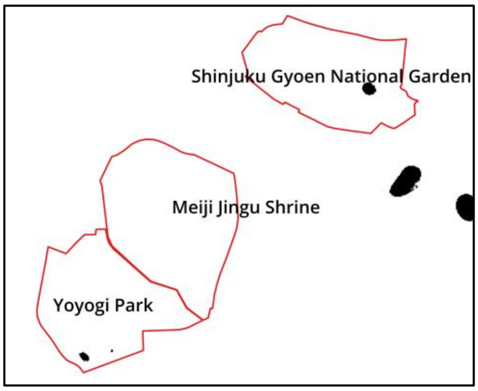

(g)

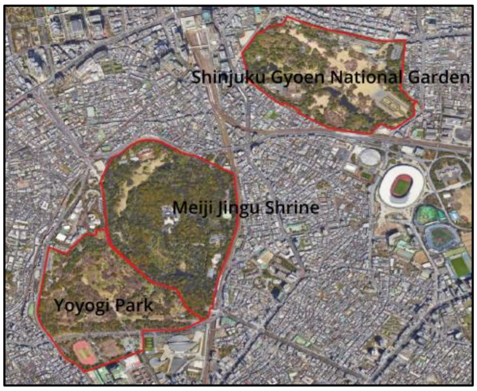

(h)

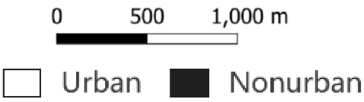

Figure 6: Close-up of omission error and commission error, (a) omission error map of proposed method, (b) omission error using raw PolSAR channels, (c) omission error using scattering decompositions, (d) optical reference from google earth, (e) commission error map of proposed method, (f) commission error using raw PolSAR channels, (g) commission error using scattering decompositions (white pixels denote urban areas, and black pixels denote nonurban areas), (h) optical reference from google earth.

Conclusion and Recommendation

This study assessed various classification methods for urban extraction using Polarimetric Synthetic Aperture Radar (PolSAR) data, comparing raw channels, scattering decomposition, and a combination of scattering decomposition with Polarimetric Orientation Angle (POA) estimation. The proposed method showed a modest improvement in accuracy, but challenges remain, particularly with commission and omission errors.

Classification based on raw channels provided a useful baseline but struggled to capture the complexities of urban environments. Scattering decomposition significantly improved classification accuracy by leveraging distinct polarimetric signatures. The inclusion of POA further enhanced results, but only marginally.

A key to the proposed method's improved accuracy was the experimental training data, which included microwave scattering characteristics from an X-band frequency. However, issues persisted, with commission errors often misclassifying parks and forests as urban, and omission errors incorrectly identifying flat surfaces like roads as non-urban.

To improve classification reliability, applying a mode filter (or majority filter) is recommended to reduce noise and ensure a smoother representation of urban features. This preprocessing step can enhance data quality and accuracy.

The findings highlight the value of advanced classification techniques in urban analysis, especially for planning and decision-making. Urban planners and researchers should prioritize methods incorporating scattering decomposition and POA while addressing the limitations related to commission and omission errors. Future research should explore multi-frequency analysis and test these methodologies in diverse urban environments to enhance their robustness and applicability.

In conclusion, while the proposed method offers slight improvements, continued refinement of classification techniques is necessary for better urban extraction using PolSAR data. Addressing these challenges will support more accurate urban mapping, contributing to the development of resilient and sustainable cities.

References

Ainsworth, T. L., Schuler, D. L., & Lee, J.-S. (2008). Polarimetric SAR characterization of man-made structures in urban areas using normalized circular-pol correlation coefficients. *Remote Sensing of Environment*, 112(6), 2885–2976.

Breiman, L. (2001). Random forests. *Machine Learning*, 45(1), 5-32.

Chaussard, E., Wdowinski, S., Cabral-Cano, E., & Amelung, F. (2014). Land subsidence in central Mexico detected by ALOS InSAR time-series. *Remote Sensing of Environment*, 140, 94-106.

Ferretti, A., Prati, C., & Rocca, F. (2000). Non-linear subsidence rate estimation using permanent scatterers in differential SAR interferometry. I*EEE Transactions on Geoscience and Remote Sensing*, 38, 2202-2212.

Ferretti, A., Fumagalli, A., Novali, F., Prati, C., Rocca, F., & Rucci, A. (2011). A new algorithm for processing interferometric data-stacks: SqueeSAR. *IEEE Transactions on Geoscience and Remote Sensing*, 49, 3460-3470.

Freeman, A. & Durden, S. L. (1998) A three-component scattering model for polarimetric SAR data. *IEEE Transactions on Geoscience and Remote Sensing*, 36, 936–973.

Kajimoto, M., & Susaki, J. (2013). Urban density estimation from polarimetric SAR images based on a POA correction method. *IEEE Journal of Selected Topics in Applied Earth Observations and Remote Sensing*, 6, 1418-1429.

Kajimoto, M., Susaki, J., & Kishimoto, M. (2020). Urban density mapping of global megacities from polarimetric SAR images. *IEEE Geoscience and Remote Sensing Letters.*

Karra, K., Kontgis, C., Statman-Weil, Z., Mazzariello, J. C., Mathis, M., & Brumby, S. P. (2021). Global land use/land cover with Sentinel-2 and deep learning. In 2021 *IEEE International Geoscience and Remote Sensing Symposium (IGARSS)*. IEEE.

Kimura, H. (2008) Radar polarization orientation shifts in built-up areas. I*EEE Geoscience Remote Sensing Letters*. 5, 217-221.

Lee, J.-S., Schuler, D. L., & Ainsworth, T. L. (2000). On the estimation of radar polarization orientation shifts induced by terrain slopes. I*EEE Transactions on Geoscience and Remote Sensing*, 40(1), 30–41.

Li, H., Li, Q., Wu, G., Chen, J., & Liang, S. (2016). The impacts of building orientation on polarimetric orientation angle estimation and model-based decomposition for multilook polarimetric SAR data in urban areas. *IEEE Transactions on Geoscience and Remote Sensing.*

Niu, X., & Ban, Y. (2012) An adaptive contextual SEM algorithm for urban land cover mapping using multitemporal high-resolution polarimetric SAR data. *IEEE Journal of Selected Topics in Applied Earth Observations and Remote Sensing*. 5, 1129-1139.

Shabou, A., Baselice, F., & Ferraioli, G. (2012) Urban digital elevation model reconstruction using very high resolution multichannel InSAR data. *IEEE Transactions on Geoscience and Remote Sensing*, 50, 4748-4758.

Yamaguchi, Y., Yajima, Y., & Yamada, H. (2006) A four-component decomposition of POLSAR images based on the coherency matrix. *IEEE Geoscience Remote Sensing Letters*, 3, 292-296.

Yamaguchi, Y. (2020). *Polarimetric SAR imaging: Theory and applications*. SAR Remote Sensing.